

River Flow Response to Precipitation and Snow Budget in California during the 1994/95 Winter

JINWON KIM AND NORMAN L. MILLER

Lawrence Berkeley National Laboratory, University of California, Berkeley, Berkeley, California

ALEXANDER K. GUETTER* AND KONSTANTINE P. GEORGAKAKOS

Hydrologic Research Center, San Diego, California

(Manuscript received 25 September 1996, in final form 29 October 1997)

ABSTRACT

A numerical study of precipitation and river flow from November 1994 to May 1995 at two California basins is presented. The Hopland watershed of the Russian River in the northern California Coastal Range and the headwater of the North Fork American River in the northern Sierra Nevada were selected to investigate the hydroclimate, snow budget, and streamflow at different elevations. Simulated precipitation and streamflow at the Hopland basin closely approximated observed values. An intercomparison between the semidistributed TOPMODEL and two versions of the lumped Sacramento model for the severe storm event of January 1995 indicates that both types of models predicted a similar response of river outflows from this basin, with the exception that TOPMODEL predicted a faster recession of river flow with less base flow after precipitation ended. Precipitation in this low-elevation watershed was predominantly in the form of rain, causing a fast streamflow response. The high-elevation Sierra Nevada watershed received most of its precipitation as snowfall. As a result, the frozen water held in surface storage delayed runoff and streamflow. Application of a simple elevation-dependent snowfall and rainfall partitioning scheme showed the significance of finescale terrain variation in the surface hydrology at high-elevation watersheds.

1. Introduction

Regional-scale hydroclimate has a significant impact on the natural environment and human activities. Specific hydrologic features such as rainfall, snowfall, and snow budget affect the frequency and duration of floods and droughts, and determine the available water resource for agriculture, urban needs, hydroelectric power production, and the health of aquatic and estuarine ecosystems. With the projected increase of human population and industrial activities, the demand for water resource will continue to increase in the future.

Accurate calculations of local hydrometeorology including precipitation, snow budget, and streamflow are particularly important for flood forecasting and reservoir operations. This capability is necessary for improving water resource management and for potentially reducing flood damages and loss of life. It is especially

important in the mountainous western United States where complex terrain, characterized by steep slopes and narrow valleys, can cause a substantial rise of river levels in a short time period during heavy precipitation events (Miller and Kim 1996). Rapid response of river flows to precipitation in mountainous areas allows for a relatively short lead time in flood warning. Efficient management of water resources depends, in part, on a combination of flood control and water storage. There is a trade-off between releases that may be viewed as lost water resources, and maintaining high reservoir water levels that may threaten the safety of dam and levee structures.

Streamflow calculations require an estimation of the amount of liquid water input to individual watersheds. Rainfall and snowmelt directly affect the amount of liquid water input to a watershed, whereas snowfall stores liquid water until there is melting. As a result, snowfall-induced runoff causes river levels to respond to precipitation with time lags ranging from a few hours to months, depending on the variation of the low-level air temperature and surface energy budget. Since a significant portion of precipitation in California is snowfall, partitioning precipitation into rainfall and snowfall and estimating the surface snow budget are important for predicting river stages (Cayan et al. 1993).

*Current affiliation: Simepar, Curitiba, Parana, Brazil.

Corresponding author address: Dr. Jinwon Kim, L-256, University of California Lawrence Berkeley National Laboratory, 1 Cyclotron Rd., Berkeley, CA 94720.
E-mail: Jinwon_Kim@lbl.gov

In the western United States, the distribution, magnitude, and phase of precipitation are strongly coupled to elevation and topography (e.g., Roads et al. 1991, 1994; Kim and Soong 1996). Moisture carried by storms from the Pacific Ocean mainly falls on the western slopes of the Coastal Range and the Sierra Nevada due to orographic lifting. Low-level moisture transport associated with the barrier jet located at the upwind side of the Sierra Nevada also causes heavy precipitation at the northern Sierra Nevada. This strong orographic forcing generates clearly defined rain shadows within the Central Valley and east of the Sierra Nevada (Kim and Soong 1996). Terrain elevation strongly affects the hydroclimate of the western United States mainly by decreasing atmospheric temperatures and increasing precipitation intensities with elevation (Cayan et al. 1993; Kim 1996; Soong and Kim 1996). At low elevations, where the surface temperature is nearly always above freezing and precipitation is mainly rainfall, rivers respond quickly to precipitation. At high elevations, snowfall dominates rainfall and surface temperature remains below freezing for longer periods, causing the precipitation to remain bound in its solid form. As the temperature rises during the spring and summer seasons, water from the melting snowpack becomes a major source of runoff. Hence the timing and amount of snowmelt are crucial for determining reservoir recharge and flood potentials. Regional temperature variation is closely related to global circulations, and regional snow budgets are affected by fluctuations in the global climate. There has been speculation that global climate variability is already affecting the timing of snowmelt-driven runoff (e.g., Roos 1991; Pupacko 1993; Dettinger and Cayan 1995). A numerical study by Jeton et al. (1996) on hydrologic responses of the North Fork American River and the East Fork Carson River has suggested that increased high-elevation precipitation would enhance snowmelt-driven spring runoff, whereas atmospheric temperature variations would modulate the timing of snowmelt over the Sierra Nevada.

Strong dependence of the wintertime precipitation and low-level air temperature on terrain elevation causes another difficulty in simulating regional hydrology. In mountainous eastern and northern California, small-scale variations in terrain elevation can cause large differences in precipitation distributions within individual basins. Terrain elevation frequently varies by 2000–3000 m within a small watershed. Since the freezing level usually appears between 1000 m and 2000 m above sea level during winter storms, using a single basin-average elevation value to compute rainfall and snowfall may cause substantial errors in computing the timing and amount of rainfall and snowfall. Direct simulation of rainfall and snowfall distributions at such fine resolutions requires extremely fine-resolution atmospheric simulations. However, it is impractical to run operational numerical weather predictions and climate simulations at such fine scales within the near future. In

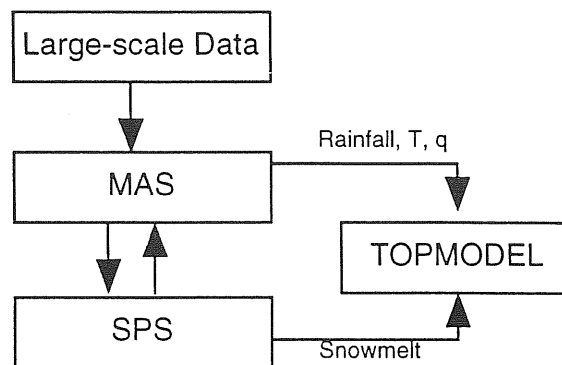


FIG. 1. Structure of the coupled atmosphere-land surface-hydrology simulation module of the RCSM.

this study, we discuss a simple elevation-dependent precipitation partitioning scheme, and the effects of sub-catchment-scale terrain elevation variation on partitioning model-simulated watershed-mean precipitation into rainfall and snowfall.

Precipitation, surface snow budget, and river flows are determined by complex interactions among many atmospheric and land surface processes at various temporal and spatial scales. Consequently, a well-designed numerical modeling system, which combines atmospheric, land surface, and hydrologic models and is coupled to large-scale atmospheric data, is an important tool for computing regional hydroclimate. We have been developing the Regional Climate System Model (RCSM) for integrated regional climate prediction and assessments of atmospheric, land surface, hydrologic, ecological, and agricultural processes at various spatial and temporal scales. In this study, we present the results of a winter season (November 1994–May 1995) hydroclimate simulation for two California watersheds using the atmospheric, land surface, and hydrologic modules of the RCSM (Kim et al. 1995). In section 2, we present brief model descriptions, in section 3 we discuss the 1995–96 hydroclimate simulations and the results are presented in sections 4–6. We also discuss a simple parameterization to account for the effects of finescale terrain elevation in simulating hydrometeorology of individual catchments at different elevations.

2. Model descriptions

The RCSM's atmospheric and land surface models are interactively coupled, and the surface hydrology-streamflow model is coupled one way (Fig. 1). Geographical information needed to map the watershed areas onto the mesoscale model domain and to provide the topographic characteristics of individual watersheds necessary for computing runoff and streamflow at each watershed are computed by the Automated Land Analysis System (ALAS; Miller 1996). The three linked numerical models are 1) the Mesoscale Atmospheric Sim-

ulation Model (MAS; Kim and Soong 1996), 2) the Soil-Plant-Snow Model (SPS; Mahrt and Pan 1984; Kim and Ek 1995), and 3) a semidistributed hydrologic model (TOPMODEL; Beven and Kirkby 1979). In addition to TOPMODEL, we are also evaluating the conceptual reservoir-type lumped Sacramento models of the National Weather Service/River Forecast Center (NWS/RFC; Burnash et al. 1973) and of the Hydrologic Research Center (HRC; Georgakakos 1986; Bae and Georgakakos 1994) to compare the performance of these two types of hydrologic models. The RCSM can be used both for regional-scale numerical weather prediction and climate simulations depending on the choice of the large-scale atmospheric forcing data. It is currently used for experimental numerical weather and streamflow predictions (Miller and Kim 1996) and assessments of regional hydroclimate and its impacts on water resources, agriculture, and ecosystems (Kim 1997; Kim et al. 1997; Miller et al. 1997). The RCSM provides daily weather and quantitative precipitation forecasts to the National Weather Service Office and the NWS/California-Nevada River Forecast Center at Sacramento, California (Kim et al. 1996). Brief descriptions of the individual models and ALAS are provided below.

The MAS model (Kim and Soong 1996) is a primitive equation limited-area mesoscale model that is equipped with an accurate third-order advection scheme (Takacs 1985) and a detailed set of parameterized physical processes. It computes convective condensation using the cumulus parameterization of Anthes (1977). The grid-scale condensation is computed by a bulk cloud microphysics scheme by Cho et al. (1989) that is based on five classes of hydrometeors (cloud water, cloud ice, rain, snow, and graupel). In this study, we employed a four hydrometeor classification (cloud water, cloud ice, rain, and snow), as the graupel concentration was negligible and the graupel processes had little impact on the simulated precipitation at the horizontal resolution used in this study.

Energy and water exchanges between the atmosphere and land surfaces are calculated interactively by the SPS model. This land surface model is based on the Oregon State University land surface model (Mahrt and Pan 1984; Pan and Mahrt 1987; Kim and Ek 1995). The SPS model predicts soil water content, soil temperature, canopy water content, and water-equivalent snow depth, but does not consider snow age or density (Anderson 1976). SPS computes temperature, water vapor mixing ratio, and snowmelt at land surfaces as a part of the surface energy balance equation. This model has successfully simulated the seasonal variations of surface energy and water budgets and soil water content at the Hydrologic Atmospheric Pilot Experiments-Modélisation du Bilan Hydrique forest site (Kim and Ek 1995) and at Cabauw, the Netherlands (Chen et al. 1997).

TOPMODEL is a spatially semidistributed hydrologic model (Kirkby 1975; Beven and Kirkby 1979). It employs topographic index values to determine the amount

of water accumulated and transported downslope within a watershed. In this study, topographic index values were derived from 3-arc-s digital elevation data. TOPMODEL computes catchment-mean values of the water table depth, soil water deficit, surface and subsurface flows, and evapotranspiration for finescale catchments. TOPMODEL assumes that 1) the dynamics of the saturated zone can be approximated as stepwise steady-state representations, 2) the hydrologic gradient follows surface topography, and 3) the downslope transmissivity is exponentially decreasing with depth. We have modified TOPMODEL so that it can be run by the MAS-SPS produced input data, including precipitation, evapotranspiration, and snowmelt.

The NWS/RFC version of the Sacramento model (Burnash et al. 1973) has been used for operational river flow predictions by RFCs around the United States. The HRC version of the Sacramento model (Georgakakos 1986; Bae and Georgakakos 1992, 1994) accounts for soil water budget, snow accumulation and ablation, frozen ground effects, and streamflow routing. The basic governing equation is the conservation of mass applied to soil water of two types (tension and gravitational) in two soil layers. Tension soil water is depleted only by vegetation and gravitational drainage flow depletes soil water from both soil layers.

ALAS is based on software developed by Jenson and Dominque (1988) and Miller (1996). It utilizes digital elevation data as input to produce flow directions and topographic characteristics at individual cells, a nested watershed numbering system at various scales, the area and location of watersheds, probability density functions (PDFs) of the topographic characteristics at each watershed, and river networks. ALAS-produced output data are necessary for computing runoff and river flow as a function of land surface characteristics.

3. Domain and experimental design

The simulation domain covers the southwestern United States region that includes California and Nevada. The MAS and SPS models are configured with a regularly spaced $20 \text{ km} \times 20 \text{ km}$ horizontal grid mesh with 14 atmospheric and two soil layers. The terrain for the MAS model was obtained by bilinearly interpolating 5-min resolution U.S. Navy terrain data. The location and topographic characteristics of selected watersheds were calculated by ALAS using 3-arc-s digital elevation data. Figure 2 illustrates the model terrain elevation and the locations of the two watersheds; the headwater of the Russian River (hereafter Hopland watershed) and the headwater of the North Fork American River (hereafter NFAH watershed). These two watersheds were selected to better understand hydrometeorology and streamflow as a function of elevation. The Hopland watershed has an area of 658 km^2 and is located between the 153- and 1158-m levels with the mean elevation of 469 m. It was selected due to its susceptibility to flooding and the

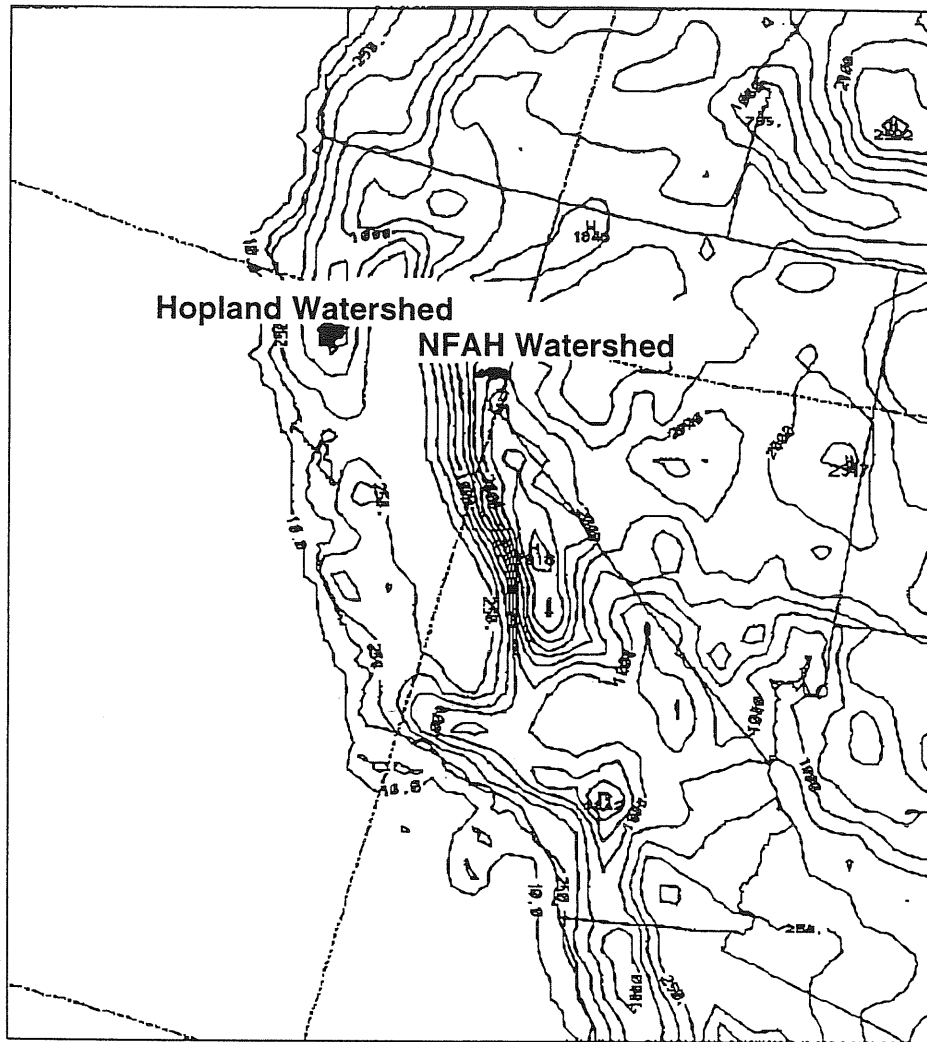


FIG. 2. Model terrain elevation at 20-km resolution. The shaded areas indicate the Hopland watershed and the NFAH watershed.

availability of river flow observations at the Hopland gauge station. The NFAH watershed area is 350 km² and has an area-weighted mean terrain elevation of 1620 m with the minimum and maximum terrain elevations of 612 and 2660 m, respectively.

Watershed-mean values of precipitation, snowmelt, and other atmospheric variables are computed from the MAS-SPS simulations by weighted-averaging of the gridpoint values. The weights for each grid box are obtained by projecting the ALAS-computed watershed area onto the model domain shown in Fig. 2. The percentage of each MAS grid cell included within a watershed area is then computed for all grid boxes within and at the boundary of a watershed. Atmospheric and land surface variables simulated by the MAS and SPS models are then averaged over the grid cells using the weights obtained from the above analysis technique.

Accuracy of regional hydrometeorological simulation

critically depends on the quality of the large-scale data that drives the regional model. We used the National Centers for Environmental Prediction Eta Model initial data at 80 km × 80 km resolution to drive this simulation from November 1994 to May 1995 at 12-h intervals. The MAS model was initialized at 0000 UTC 3 November 1994. After we began the simulation, lateral boundary conditions obtained from the twice-daily Eta Model initial fields were provided to the MAS model for the 7-month period to provide the time-dependent large-scale forcing. The SPS model was initialized using the November climatology of soil water content obtained from Zabler (1986). Even though this climatological data does not accurately represent the initial soil moisture content, heavy precipitation at the beginning of this winter season would quickly spin up the near-surface soil moisture field as suggested by the sensitivity study of Kim and Ek (1995).

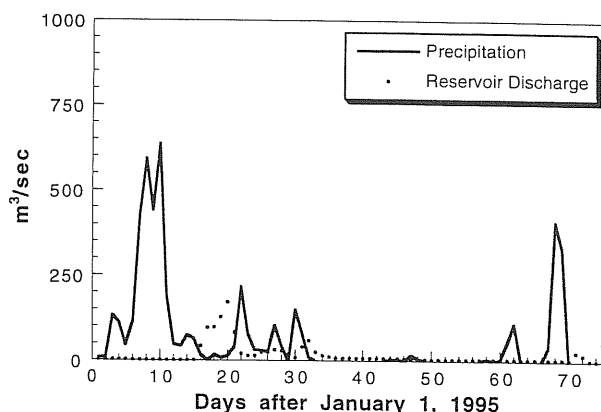


FIG. 3. Liquid water input to the Hopland watershed during 1 Jan–15 Mar 1995. The solid line indicates the simulated precipitation integrated over the watershed area ($\text{m}^3 \text{s}^{-1}$) and the dots represents the reservoir discharge rate.

4. Precipitation and streamflow at a low-elevation watershed: Hopland

The simulated watershed-mean precipitation at the Hopland watershed is presented in Fig. 3 together with the amount of water released by the upstream Coyote reservoir. Miller and Kim (1996) showed that the simulated precipitation agrees well with observations during the 12-day period in early January 1995. Missing rain gauge data at the stations used for computing the watershed-mean precipitation prevented a comprehensive evaluation of simulated precipitation for a longer period. Figure 3 shows that discharge of water from the upstream reservoir is another major source of river flow variation at the Hopland river gauge station especially during low flow periods and before anticipated storms (e.g., near day 20 in Fig. 5a). Snowfall (not shown) was negligible within this watershed, except during the late March 1995 storm when the freezing level dropped below the 200-m level.

Figure 4 illustrates the TOPMODEL-simulated and observed daily mean river flows at the Hopland river gauge station for a 75-day period from 1 January to 15 March 1995. We selected this period due to the avail-

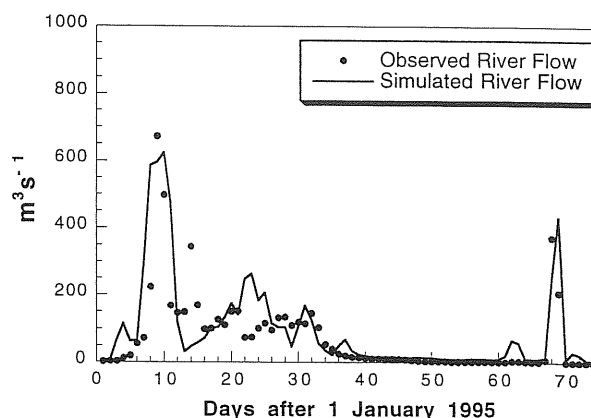


FIG. 4. The observed (solid dots) and simulated (dashed line) river flow from 1 Jan to 15 Mar 1995 at the Hopland gauge station.

ability of daily discharge records from the upstream Coyote reservoir as it is the predominant source of river flow during nonprecipitating periods. We calibrated TOPMODEL for the Hopland watershed using the observed records of precipitation and streamflow for the 1962–82 period. The optimization scheme by Rosenbrock and Storey (1966) was used to obtain the hydraulic conductivity and scaling parameters. The TOPMODEL parameters for the Hopland watershed are presented in Table 1. We assumed that the soil of the basin was 85% saturated after two storms prior to the beginning of the simulation.

The simulated streamflow at the Hopland gauge station agrees closely with the observed values, especially during the periods of heavy precipitation in January and March 1995 (Fig. 4). The simulated streamflow results during early January 1995 flooding along the Russian River were presented in Miller and Kim (1996). The difference between the simulated and observed river flows is less than 10% of the observed streamflow during the high flow periods of early January and March 1995. We attribute these good results to the near-saturated soil conditions prior to the beginning of the simulation. As snowfall is negligible below the 1000-m level, streamflow at the Hopland watershed quickly re-

TABLE 1. User-specified TOPMODEL parameters used to compute river flow at the Hopland watershed (1994).

Parameter (unit)	Description	Hopland watershed
m (mm)	Scaling parameter	5.50
K (mm day^{-1})	Saturated hydraulic conductivity of C soil horizon	250.0
P_{macro}	Ratio of precipitation bypassing soil zone	0.0
Z_{tot} (m)	Total soil depth	1.0
Z_{ub} (m)	Upper soil depth	0.05
θ_{fc}	Field capacity	0.35
M_A [$\ln(\text{m})$]	Mean topographic index	6.61
V_A [$\ln(\text{m}^2)$]	Variance of topographic index	2.05
S_A [$\ln(\text{m}^3)$]	Third moment of topographic index at maximum vertical gradient	3.73
A	Total watershed area	658.0
T_{cut} ($^{\circ}\text{F}$)	Cutoff temperature for snowmelt	32.0
P_{imp}	Ratio between the impervious area and the total watershed area	0.01

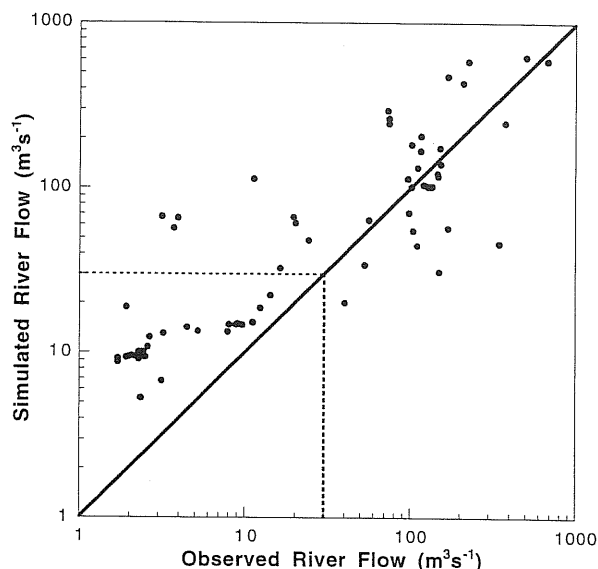


FIG. 5. A comparison of the simulated (vertical) and observed (horizontal) daily mean river flow rate at the Hopland gauge station. The solid line indicates exact agreements between the simulated and observed river flows.

sponded to individual precipitation events and the reservoir discharge. Within this watershed, streamflow is delayed predominantly by the time required to saturate the near-surface soil layer. During the wet winter season, the near-surface soil layer was nearly saturated due to frequent precipitation. Hence, any significantly delayed response of streamflow to precipitation was absent in both observed and simulated streamflow, as was previously discussed by Cayan et al. (1993).

Figure 5 shows that the simulated streamflow agrees well with the observed values above and below $30 \text{ m}^3 \text{ s}^{-1}$. Below $30 \text{ m}^3 \text{ s}^{-1}$, TOPMODEL significantly over-predicts observations. This discrepancy between the simulated and observed streamflows during low flow periods may be caused by the assumptions that the hydraulic gradient parallels the surface topographic gradient and that the hydraulic conductivity is horizontally uniform within the watershed and decreases exponentially with increasing depth. Uncertainties in the streamflow and reservoir discharge records also have potentially contributed to the discrepancy, as reservoir discharge is the main source of streamflow during the non-precipitating period. Investigation of streamflow and reservoir discharge records shows that during low flow periods, reservoir discharge sometimes exceeds the recorded river flow. This uncertainty in the river flow and reservoir discharge records prevented us from making a comprehensive evaluation of model simulation during low flow periods. We are currently recalibrating TOPMODEL in conjunction with a streamflow router, constructing a fine-resolution soil information database for major California watersheds, and are working to incorporate recent generalizations of the TOPMODEL as-

sumptions, including various formulations of the hydraulic conductivity (Ambroise et al. 1996; Duan and Miller 1997).

Large-scale watersheds have been usually simulated by lumped models (e.g., operational river flow prediction by the NWS/RFC using the Sacramento model). Distributed models may be used for small watersheds, provided that sufficiently fine-resolution digital elevation model data and soil characteristic data are available. For most watersheds, soil characteristics such as the spatial variation of soil texture, depth of the upper soil layer, and the amount of soil water flowing into deep aquifers, are not well quantified. As a result, use of distributed hydrologic models to compute river flow at large watersheds needs careful evaluation. As an example, in Fig. 6 we compare 6-h river flows simulated by TOPMODEL and two types of the Sacramento model (RFC- and HRC-version) against the 6-h river gauge observations from 1 to 21 January 1995 using precipitation simulated by the MAS-SPS model. Spinup and calibration of the two lumped models were made using the same historical precipitation and river flow data as for TOPMODEL. Parameters for the RFC and HRC versions of the Sacramento model were estimated from daily data and are presented in Table 2. Comparison of 6-h simulations to the observation ended at 11 January, since 6-h dam release records were not available. All three hydrologic models simulated the peak flow as occurring on early January 9. The major difference in the three hydrologic model results appears during the recession after the storms ended. All three models simulated a much slower recession than observed. The observation shows that after the peak flow, streamflow decreases quickly to about $170 \text{ m}^3 \text{ s}^{-1}$ after 48 h. The two lumped models predicted streamflow at $200 \text{ m}^3 \text{ s}^{-1}$, whereas TOPMODEL simulated streamflow at $100 \text{ m}^3 \text{ s}^{-1}$ after 48 h. All three models predicted that near-steady streamflow conditions occur about 100 h after the peak flow has occurred. However, TOPMODEL-simulated base flow drops to near zero and the two lumped models predicted much higher base flow values. The initial steep decrease of river flow is typically associated with the cessation of surface runoff and the depletion of near-surface soil water, whereas the slower decrease of the hydrograph is associated with the production of base flow and the depletion of deep soil water. From this point of view, all three models predicted much slower depletion of near-surface soil water during the initial recession period.

5. Precipitation and river flow at a high-elevation watershed: NFAH

In this section, we present the simulated hydrometeorology of the NFAH basin. Since historical records of precipitation and river gauge data are not available for this small headwater watershed, we calculated only TOPMODEL parameters that are dependent upon ter-

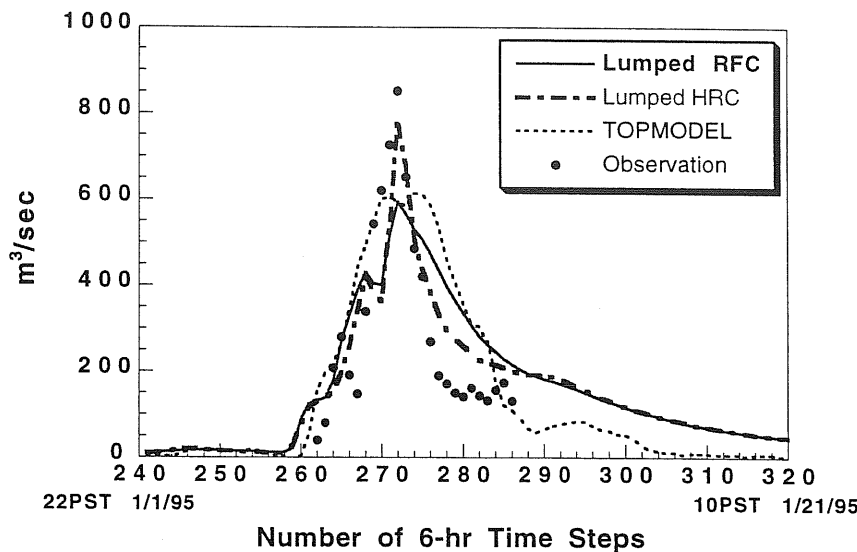


FIG. 6. Six-hourly river flow at the Hopland gauge station simulated by TOPMODEL and RFC and HRC versions of the Sacramento model.

rain elevation (e.g., topographic index). Other parameters such as soil depth and hydraulic conductivity are adapted from the Hopland watershed values. As a result, we discuss only the qualitative features of the hydroclimate at high-elevation watersheds derived from the simulated precipitation and river flow.

Because of its high elevation, snowfall dominates rainfall at this watershed (Fig. 7). During winter storms, the freezing level is usually located between the 1000- to 2000-m levels. Hence, the mean elevation of this watershed is located mainly above the freezing level during winter storms. Even during the warm storms of early January 1995 (near day 70 in Fig. 7) when the freezing level was occasionally as high as 2000 m, daily rainfall was less than 40% of daily snowfall. The percent of rainfall to snowfall increases toward the end of the winter season with a general increase in atmospheric temperature. During the storms in late April and early May 1995 (near day 180 in Fig. 7), the rainfall intensity was comparable to the snowfall amount.

As a consequence of this rainfall and snowfall distribution, water from melting snow is the dominant source of streamflow at this high-elevation watershed. One of the important roles of the snow budget within this high-elevation watershed is the delay of the impact of precipitation on surface runoff and streamflow. Streamflow at high-elevation watersheds (Fig. 8) is a strong function of snowmelt and seasonal temperature variations (Cayan et al. 1993; Jeton et al. 1996). Snowpack stores water until the surface temperature warms sufficiently. This lag between snowfall and river response is seen in Fig. 8. During May, the river rises in response to the increasing snowmelt rate. This predictive capability will become a useful tool for water resources management if a precipitation and streamflow

database becomes available for calibration and validation of the modeling system.

6. Elevation-dependent precipitation type distribution at NFAH

Partitioning between rainfall and snowfall and the surface snow budget plays a major role in determining the timing and amount of river flow at high-elevation watersheds. The surface snow budget is a function of snowfall and the surface energy budget. It strongly depends on the elevation of the snowline and low-level air temperature. In mountainous northern and eastern California, terrain elevation varies significantly at small scales. Neglecting the finescale elevation variation in calculating rainfall and snowfall, however, can cause significant errors in the surface hydrology calculations. Figure 9 illustrates the distribution of terrain elevation for the NFAH watershed where the terrain elevation varies from 612 to 2660 m with an area-weighted mean elevation of 1620 m. The resulting terrain-elevation PDF (solid line with open circles) and the cumulative PDF (CPDF) are convenient tools for computing the portion of the land surface area below a certain elevation. For example, in Fig. 9, the elevation of 1620 m corresponds to the CPDF value of 0.5, which implies that 50% of this watershed area is located below the 1620-m level. The terrain elevation corresponding to CPDF = 0.5 is also the area-weighted watershed-mean elevation. Multiplying the precalculated total watershed area by a CPDF value yields the area below the prescribed elevation.

Figure 10 shows the simulated daily mean freezing level for the NFAH watershed from 1 March to 31 May 1995. Our discussion is limited to this period because

TABLE 2. Parameters for the RFC and HRC versions of the Sacramento models. Nomenclature follows Bae and Georgakakos (1994).

Parameter (unit)	Description	RFC	HRC
x_1^0 (mm)	Upper soil tension water capacity	91.00	36.70
x_2^0 (mm)	Upper soil free water content	30.00	101.70
x_3^0 (mm)	Lower soil tension water capacity	127.00	380.70
x_4^0 (mm)	Lower soil free water capacity	35.00	35.00
x_5^0 (mm)	Lower soil supplementary free water capacity	74.00	74.00
d_u (day ⁻¹)	Interflow coefficient	0.480	0.272
d' (day ⁻¹)	Primary baseflow coefficient	0.006	0.006
d'' (day ⁻¹)	Supplementary baseflow coefficient	0.150	0.150
ε	Coefficient of increase in percolation at maximum vertical gradient	8.00	65.00
θ	Exponent in percolation function for unsaturated soil	1.90	1.90
P_f	Fraction of free percolated water	0.20	0.20
μ	Baseflow fraction not flowing through basin outlet	0.00	0.02
β_1	Maximum fraction of impervious area	0.043	0.043
β_2	Fraction of permanently impervious area	0.005	0.005
α (day ⁻¹)	Coefficient of upland routing reservoirs	6.510	6.510

the time-mean temperature used to compute the freezing level was not available before this period. Note also that the watershed-mean model terrain is located at the 1896-m elevation for this watershed. This 276-m difference between the fine-resolution area-mean elevation (1620 m) and the atmospheric model terrain (1896 m) is due to the interpolation of a coarse-resolution terrain data (5 arc-min) and smoothing to obtain the atmospheric model terrain. When subcatchment-scale elevation variation is not considered, the atmospheric model provides precipitation to river flow models in such a way that if the freezing level is above the model terrain (dashed line in Fig. 10), the area-mean precipitation is entirely rain. In the opposite case, the entire precipitation is provided to the river model as snow. This method can cause

a significant error in the rainfall and snowfall distribution within this NFAH watershed since the freezing level is located within the range of terrain elevation variation throughout the winter season.

To improve rainfall and snowfall distributions within high-elevation watersheds, we devised a simple precipitation-partitioning scheme utilizing the terrain elevation CPDF (Fig. 9) and the location of the simulated freezing level (Fig. 10). This scheme is analogous to that described by WMO (1994) but has not been widely used in atmospheric research. In this simple scheme, the amount of rainfall and snowfall over a watershed at a given time is computed in such a way that the portion of the precipitation below (above) the freezing level is rainfall (snowfall). Figures 11a and 11b compare the

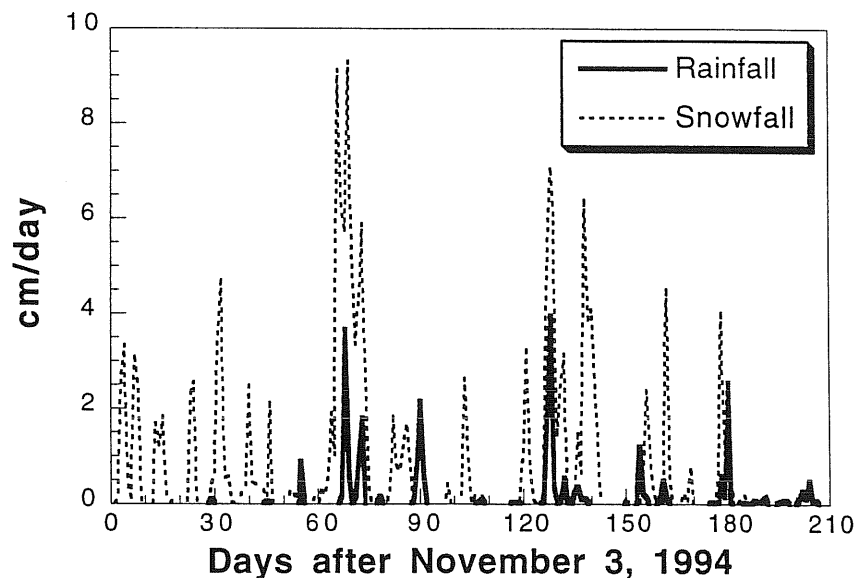


FIG. 7. The simulated watershed-mean daily rainfall (solid line with open circles) and daily snowfall (dashed line with solid circles) at the NFAH watershed for the period from 3 November 1994 to 31 May 1995.

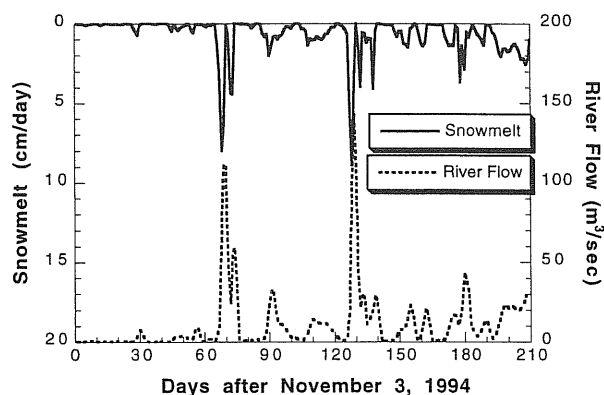


FIG. 8. The simulated daily snowmelt and daily mean river flow at the NFAH watershed. The period of presentation is the same as Fig. 6.

rainfall and snowfall distribution computed by the watershed-mean terrain elevation (solid line) against that computed by using the above elevation-dependent partitioning scheme (dashed line). These two methods yield quite different rainfall and snowfall partitioning for this high elevation watershed. When subcatchment-scale terrain variation is included in partitioning precipitation into rainfall and snowfall, the amount of the calculated snowfall (rainfall) within this watershed is significantly reduced (increased). This is further complicated by the dependence of precipitation amounts on terrain elevation as shown by Leung and Ghan (1995) and Kim (1998). We are further developing this scheme to include the elevation-dependence of precipitation amount, surface energy balance, snow budget, and streamflow.

7. Conclusions

Wintertime hydrometeorology, surface snow budget, and streamflows at two California watersheds, the Hopland watershed at the northern Coastal Range and the headwater of the North Fork American River basin at the northern Sierra Nevada, were simulated for the 7-month period of November 1994–May 1995 using the Regional Climate System Model. One of the goals of this study was to downscale the large-scale weather information to the catchment scales using a mesoscale model and fine-resolution geographic information data. This has been achieved with a reasonable success, even though there is room for improvements. The simulated area-mean precipitation and river flow at the Hopland watershed agree well with the observed values during the early 1995 period when the reservoir discharge records and river flow observations were available. Overall, the simulated river flow showed better than 50% accuracy and better than 90% accuracy during high river flow periods at this low-elevation watershed.

The simulated hydrometeorology, snow budget, and river flows strongly depend on the terrain elevation due to the variations of precipitation type and snowmelt as

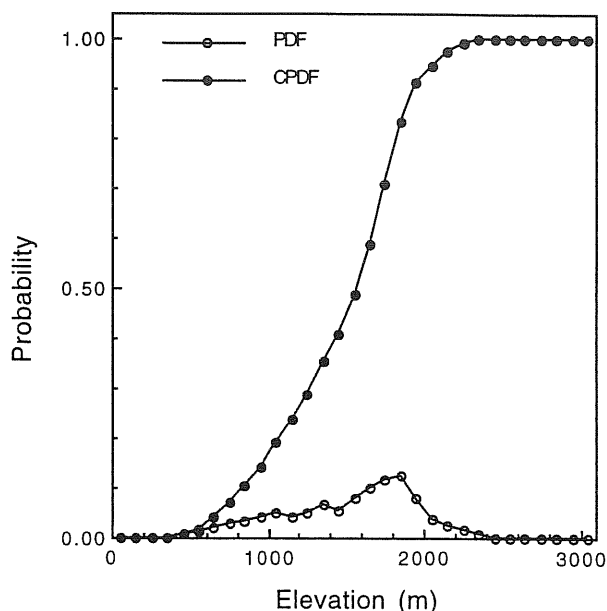


FIG. 9. The probability distribution function (PDF; solid line with open circles) and the cumulative probability distribution function (CPDF; dashed line with solid circles) of finescale terrain elevation at the NFAH watershed.

a function of terrain height. Rainfall dominates snowfall at low-elevation watersheds, causing river flow originating from the Hopland watershed to respond quickly to precipitation events. Reservoir operation appears to be the major factor that controls the river flow volume during nonprecipitating periods. Snow budget appears to be the major factor that determines river flows at high-elevation watersheds. Streamflow at the headwater

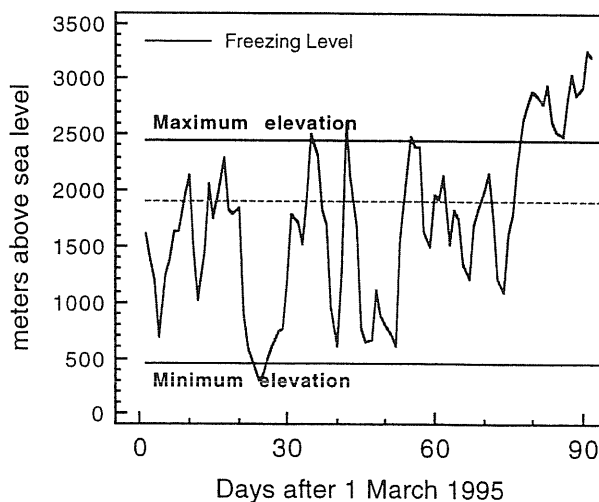


FIG. 10. Elevation of the daily mean freezing level at the NFAH watershed for March–May 1995 period. The horizontal dashed line at constant 1900 m indicates the value of model terrain elevation. The other two horizontal solid lines at 2450 m and 450 m indicate the maximum and minimum elevation within the watershed.

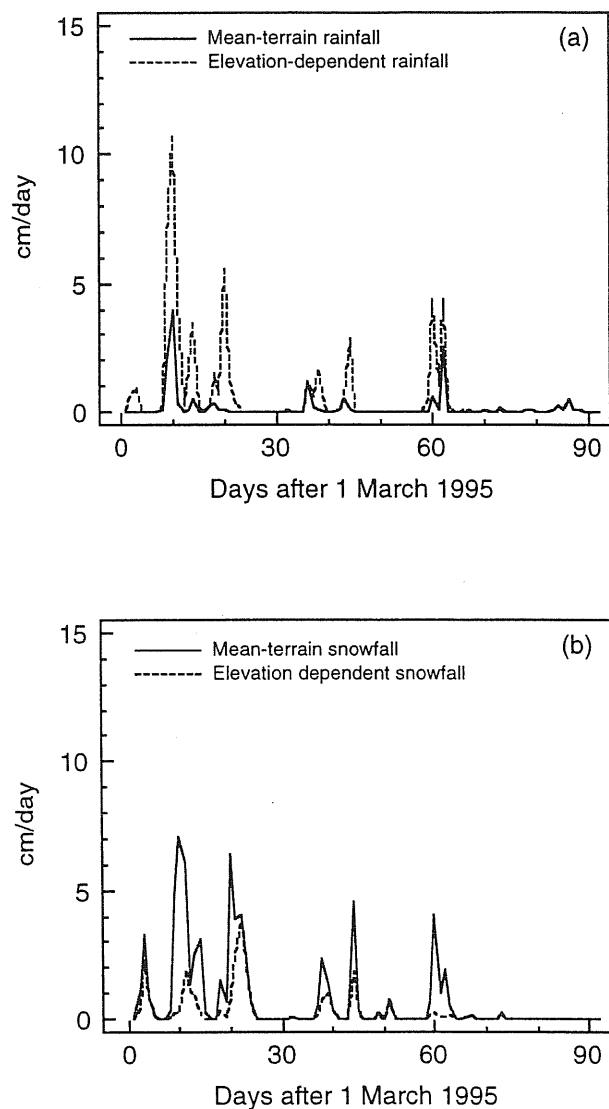


FIG. 11. The simulated 6-h rainfall (a) and snowfall (b) at the NFAH watershed. The solid (dashed) lines indicate the rainfall and snowfall values simulated without (with) considering the subcatchment-scale elevation variation.

of the North Fork American River (mean elevation of 1620 m) showed a delayed response to precipitation due to large amounts of snowfall during the wintertime. Most of the spring runoff from this basin came from snowmelt.

One of the difficult parts of coupled hydrometeorological modeling over mountainous regions is accounting for the effects of finescale terrain variation on precipitation and hydrology. Consideration of low atmospheric temperature variation due to subgrid-scale terrain variation suggests that subcatchment-scale elevation variation has a significant impact in partitioning the simulated precipitation into rainfall and snowfall. When we applied a simple elevation-dependent pre-

cipitation partitioning scheme to the NFAH watershed, the rainfall and snowfall distribution within the watershed changed significantly. It is further complicated as terrain elevation also affects the amount of local precipitation (Leung and Ghan 1995; Kim 1997). Dependence of precipitation on terrain elevation may be a complex function of the spatial scale of terrain variation, elevation, and the large-scale storm environment and associated cloud microphysics. We are currently developing an elevation-dependent precipitation partitioning scheme that includes the effects of subbasin terrain variation on precipitation distribution, surface snow budget, and surface energy budget.

Proper scales of hydrologic response units for streamflow calculations is another important issue to be studied for downscaling atmospheric data and streamflow calculations. As the size of a hydrologic response unit increases, we can better define area-averaged atmospheric forcing for each area. On the other hand, large hydrologic units may cause problems with spatially distributed models such as TOPMODEL. To resolve this, we are developing a scheme to compute streamflow over a large-scale basin using TOPMODEL and a streamflow router in anticipation of fine-resolution precipitation simulation.

Acknowledgments. We thank the staff of the NOAA/NWS California-Nevada River Forecast Center for the river flow data. We also thank H. Walker, J. Duan, and the EROS data center for the digital elevation data. This work was supported by the Laboratory Directed Research and Development and University of California Campus Laboratory Collaboration project. The work of the last two authors was supported by the NOAA Experimental Climate Prediction Center of the Scripps Institution of Oceanography. The Livermore Computing, the San Diego Supercomputing Center, and the Atmospheric Release Advisory Capability provided the computational resources. This work was performed under the auspices of the U.S. Department of Energy by Lawrence Livermore National Laboratory under Contract W-7405-Eng-48.

REFERENCES

- Ambrose, B., K. Beven, and J. Freer, 1996: Toward a generalization of the TOPMODEL concepts: Topographic indices of hydrological similarity. *Water Resour. Res.*, **32**, 2135–2145.
- Anderson, E. A., 1976: A point energy and mass balance model of a snow cover. NOAA Tech. Rep. NWS 19, Office of Hydrology, NWS, Silver Spring, MD, 150 pp.
- Anthes, R., 1977: A cumulus parameterization scheme utilizing a one-dimensional cloud model. *Mon. Wea. Rev.*, **105**, 270–286.
- Bae, D.-H., and K. P. Georgakakos, 1992: Hydrologic modeling for flow forecasting and climate studies in large drainage basins. Department of Civil and Environmental Engineering and Iowa Institute of Hydrologic Research Rep. 360, Hydrologic Research Center, La Jolla, CA, 252 pp.
- , and —, 1994: Climatic variability of soil water in the American midwest. Part 1: Hydrologic modeling. *J. Hydrol.*, **162**, 355–377.

- Beven, K., and M. Kirkby, 1979: A physically based, variable contributing area model of basin hydrology. *Hydrol. Sci. Bull.*, **24**, 43–69.
- Burnash, R., R. Ferral, and McGuire, 1973: A generalized streamflow simulation system—conceptual modeling for digital computers. Tech. Rep., NOAA, NWS, and State of California, Dept. of Water Resources, Joint Federal-State River Forecast Center, Sacramento, CA, 204 pp.
- Cayan, D., L. Riddle, and E. Aguado, 1993: The influence of precipitation and temperature on seasonal streamflow in California. *Water Resour. Res.*, **29**, 1127–1140.
- Chen, T., and Coauthors, 1997: Cabauw experimental results from the Project for Intercomparison of Land-surface Parameterization Schemes (PILPS). *J. Climate*, **10**, 1194–1213.
- Cho, H., M. Niewiadomski, and J. Iribarne, 1989: A model of the effect of cumulus clouds on the redistribution and transformation of pollutants. *J. Geophys. Res.*, **94** (D10), 12 895–12 910.
- Dettinger, M., and D. Cayan, 1995: Large-scale atmospheric forcing of recent trends toward early snowmelt runoff in California. *J. Climate*, **8**, 606–623.
- Duan, J., and N. Miller, 1997: A generalized power function for the subsurface transmissivity profile in TOPMODEL. *Water Resour. Res.*, **33**, 2559–2562.
- Georgakakos, K. P., 1986: A generalized stochastic hydrometeorological model for flood and flash flood forecasting. Part 1: Formulation. *Water Resour. Res.*, **22**, 2083–2095.
- Jenson, S., and J. Dominique, 1988: Extracting topographic structure from digital elevation data for geographic information system analysis. *Photogramm. Eng. Remote Sens.*, **54**, 1593–1600.
- Jeton, A. E., M. D. Dettinger, and J. L. Smith, 1996: Potential effects of climate change on streamflow, eastern and western slopes of the Sierra Nevada, California and Nevada. Water Resources Investigations Rep. USGS 95-4260, 44 pp.
- Kim, J., 1996: Numerical simulation of precipitation over the southwestern United States during the 1994–1995 winter season. Preprints, *Symp. on Environmental Applications*, Atlanta, GA, Amer. Meteor. Soc., 176–179.
- , 1998: Precipitation and snow budget over the southwestern United States during the 1994–1995 winter season. *Water Resour. Res.*, in press.
- , and M. Ek, 1995: A simulation of the long term surface energy budget and soil water content over the HAPEX-MOBILHY forest site. *J. Geophys. Res.*, **100** (D10), 20 845–20 854.
- , and S.-T. Soong, 1996: Simulation of a precipitation event in the western United States. *Regional Impacts of Global Climate Change*, S. J. Ghan, W. T. Pennel, K. L. Peterson, E. Rykiel, M. J. Scott, and L. W. Vail, Eds., Battelle Press, 73–84.
- , —, O. Rhea, and N. Miller, 1995: A numerical prediction of the precipitation and hydrology of California. Preprints, *14th Conf. on Weather Analysis and Forecasting*, Dallas, TX, Amer. Meteor. Soc., 230–234.
- , N. Miller, S. Cunningham, O. Rhea, and E. Strem, 1996: Quantitative precipitation and river flow predictions over the southwestern United States. Preprints, *11th Conf. on Numerical Weather Prediction*, Norfolk, VA, Amer. Meteor. Soc., J133–J135.
- , —, J.-S. Chung, and J.-H. Oh, 1997: A simulation of precipitation and land-surface water budget over the East Asia using the UC-LLNL Regional Climate System Model. *Third International Study Conference on GEWEX/GAME*, International GEWEX Project Office Publication Series No. 24, World Climate Research Programme, 265.
- Kirkby, M., 1975: Hydrograph modelling strategies. *Process in Physical and Human Geography*, R. Reel, M. Chisholm, and P. Haggett, Eds., Heinemann, 69–90.
- Leung, L. R., and S. J. Ghan, 1995: A subgrid parameterization of orographic precipitation. *Theor. Appl. Climatol.*, **52**, 95–118.
- Mahrt, L., and H.-L. Pan, 1984: A two-layer model simulation of soil hydrology. *Bound.-Layer Meteor.*, **29**, 1–20.
- Miller, N. L., 1996: An Automated Land Analysis System (ALAS) for applications at a range of spatial scales: Watershed to global. *Next Generation Environmental Models and Computational Methods*, G. Delic and M. F. Wheeler, Eds., SIAM, 169–173.
- , and J. Kim, 1996: Numerical prediction of precipitation and river flow over the Russian River watershed during the January 1995 California storms. *Bull. Amer. Meteor. Soc.*, **77**, 101–105.
- , —, J.-S. Chung, J.-H. Oh, and D.-H. Bae, 1997: East Asian hydroclimate and agro-ecosystem research using the UC-LLNL Regional Climate System Model. *Third International Study Conference on GEWEX/GAME*, International GEWEX Project Office Publication Series No. 24, World Climate Research Programme, 153–158.
- Pan, H.-L., and L. Mahrt, 1987: Interaction between soil hydrology and boundary layer development. *Bound.-Layer Meteor.*, **38**, 185–202.
- Pupacko, A., 1993: Variations in northern Sierra Nevada streamflow: Implications of climate change. *Water Resour. Bull.*, **29**, 283–290.
- Roads, J. O., N. Maisel, and J. Alpert, 1991: Further evaluation of the National Meteorological Center's Medium Range Forecast Model prediction forecasts. *Wea. Forecasting*, **6**, 483–497.
- , S.-C. Chen, A. K. Guetter, and K. P. Georgakakos, 1994: Large-scale aspects of the United States hydrologic cycle. *Bull. Amer. Meteor. Soc.*, **75**, 1589–1610.
- Roos, M., 1991: Trend of decreasing snowmelt in northern California. Preprints, *59th Annual Western Snow Conf.*, Juneau, AK, Western Snow Conference, 19–38.
- Rosenbrock, H., and C. Storey, 1966: *Computational Techniques for Chemical Engineers*. Pergamon Press, 328 pp.
- Soong, S.-T., and J. Kim, 1996: Simulation of a heavy precipitation event in California. *Climate Change*, **32**, 55–77.
- Takacs, L., 1985: A two-step scheme for the advection equation with minimized dissipation and dispersion errors. *Mon. Wea. Rev.*, **113**, 1050–1065.
- WMO, 1994: *Guide to Hydrological Practices*. 5th ed. WMO-168, 735 pp.
- Zobler, L., 1986: A world soil file for global climate modeling. NASA Tech. Memo. 87802, 32 pp. [Available from Goddard Institute for Space Studies, New York, NY 10025.]